International Journal of Production Research, 2018
Vol. 56, No. 3, 1269–1285, https://doi.org/10.1080/00207543.2017.1395487

Power-load management reduces energy-dependent costs of multi-aisle mini-load automated storage and retrieval systems

Paul Hahn-Woernle[a,b]* and Willibald A. Günthner[a]

[a]*Lehrstuhl für Fördertechnik Materialfluss Logistik (Institute for Materials Handling, Material Flow, Logistics), Technische Universität München, Garching, Germany;* [b]*viastore SYSTEMS GmbH, Stuttgart, Germany*

(*Received 18 November 2015; accepted 6 October 2017*)

For economic and ecological reasons, the interest in the energy demand of material-handling systems is rising. As a result, the operators of these systems increasingly pay attention to the energy demand and the costs resulting from it. The energy demand of automated warehouses, with multi-aisle automated storage and retrieval systems, is volatile with uncontrolled power-peaks. These power-peaks result in high energy and hardware costs. In this paper, the effect of a power-load management on the throughput of the material-handling systems is investigated. We assume that the peaks of energy consumption can be significantly reduced by delaying tasks, without having an impact on the throughput. The goal is to find out the interdependence between the electrical power-limits of the power-load management (mean power demand in a period and maximum power demand) and the throughput of the warehouse. The results show that, with a maximum power-limit and a mean power-limit, the peaks in energy consumption can be avoided with only a slight loss of throughput. Load management is an effective method to reduce the energy peaks of an automated warehouse, thereby lowering the costs of automated warehouses.

Keywords: automated storage; AS/RS; material-flow; parallel machines; simulation; performance analysis; power-load management; storage and retrieval machines; multi-aisle AS/RS

1. Introduction

On the one hand, globalisation gives companies the chance to enter new markets, gain new customers and access a wider selection of suppliers but, on the other, it also exposes companies to greater competitive and financial pressure. Handling new suppliers and new markets, as well as surviving in the competition, requires successful supply chain management; this includes the optimisation of logistic processes. These processes can be divided into 'transport logistics' and 'intralogistics'. 'Transport logistics' is the logistics between supply chain hubs. 'Intralogistics' is the logistics inside a hub combined with the related global information flow. Intralogistics systems are also called material-handling systems.

Highly effective material-handling systems (high throughput at low costs) are mostly highly automated computer-controlled systems. Due to the rising costs of electricity, electricity charges contribute an ever increasing proportion of their lifecycle costs: thus, the ROI and the efficiency decrease.

Additional costs arise through oversized electrical hardware (e.g. transformers, cables…), which is designed for the worst-case power peaks, and through higher energy costs, which are caused by higher peak loads (highest energy consumption in a specified time period – in Germany 15 min – over a billing cycle). These energy-dependent costs can be reduced by downsizing the hardware and limiting the peak loads.

An effective way to reduce costs (both in energy and hardware) is to avoid volatile energy consumption. This can be achieved with a power-load management (PLM) that prevents peaks in the energy consumption by delaying energy-consuming processes (e.g. machine movements). In this study, the PLM prevents peaks of the multi-aisle automated storage and retrieval system (MA-AS/RS) by delaying its tasks (e.g. travel to location X/Y). However, for the operator of a material-handling system, the throughput of the system has the highest priority. For the strategies of a PLM system to be accepted by the operators, it has to be shown that the PLM does not impact the throughput of MA-AS/RS.

In this paper, the impact of the PLM on the throughput of a mini-load MA-AS/RS is studied. Therefore, a simulation model is built to simulate their behaviour and energy consumption. With this model, the dependencies between the system throughput and the level of the energy-demand limits of the PLM are identified. There are two energy-demand

*Corresponding author. Email: pa.hahn-woernle@viastore.com

limits: a maximum power-limit (MAL) and a mean power-limit (MEL; limit for the mean electrical power consumption over a period of 15 min). This study focuses on automated warehouses with MA-AS/RS because of their highly volatile energy consumption. Multiple parallel storage and retrieval machines (SRM) are investigated, so that electrical load-balancing is possible. With the results, the operators can see that PLM is an effective way to prevent unintentional power peaks and energy-dependent costs.

This paper is structured as follows. Section 2 gives a brief introduction to the topics of this paper and reviews the related literature. The assumptions are described in Section 3, followed by an overview of the simulation model in Section 4. The Sections 5 and 6 describe the simulation model controllers, and the SRM power calculation model, respectively. In Section 7, the PLM model is described in detail, followed by the calibration and validation of the simulation model in Section 8. In Section 9, the simulation is introduced and the simulation results are discussed. Finally, Section 10 concludes this paper and gives recommendations for further research.

2. Background and literature review

This chapter provides an introduction to the topics of warehousing, power-load management and energy costs, followed by the literature review.

2.1 *Warehousing and SRM*

Warehouses are an important component in the supply chain for buffering, consolidation, commissioning and value-added processes. For the storage of totes in the warehouse, autonomous vehicle storage and retrieval systems (AVS/RS) or AS/RS can be used. While AVS/RS are best for small warehouses with a high throughput, AS/RS are used for large warehouses with an average throughput (Lerher, Edl, and Rosi 2014, 98). Due to their volatile energy demand, AS/RS are investigated in this paper.

AS/RS normally consist of two storage-racks, an SRM moving in the aisle between them and one input and output location (I/O). For a single-cycle storage (FEM 9.851 2003), the SRM picks up a tote at the I/O, moves it to a location, stores it there and drives back to the I/O. A single-cycle retrieval is the reverse process. For a combined cycle, the SRM picks up a tote at the I/O, moves it to the storage location, stores it there, travels to the retrieval location, retrieves the retrieval tote from there and delivers it to the I/O. With a double-deep SR, the tote is sometimes blocked by another tote, thus the blocking tote has to be relocated to retrieve the blocked tote. This process is called relocation. The overall time of the combined cycle is the sum of the times for the movements ($t_{IOP1}, t_{P1P2}, t_{P2IO}$) and the sum of times for the storing and retrieving of the totes (t_{02}; times for positioning, load-handling device (LHD) movements, etc.). The cycle time is calculated as follows (FEM 9.851 2003):

$$t_C = t_{IOP1} + t_{P1P2} + t_{P2IO} + t_{02} \tag{1}$$

The throughput is 'the mean unit load flow in to and out of the warehouse' (Verein Deutscher Ingenieure 1998) and dependent on the cycle time. To calculate the throughput, the amount of cycles Z_c (e.g. combined cycles) is divided by the time demand to execute those cycles t_c (Verein Deutscher Ingenieure 1998). Usually, the throughput (here of combined cycles) is given as the amount of cycles per hour:

$$Q_C = \frac{Z_c}{t_c} \tag{2}$$

Thus, in this paper, the throughput of an SRM is specified in the number of storages and retrievals per hour and not separated into the different types of cycles.

2.2 *Power-load management – PLM*

A PLM is a system used to avoid peaks of electricity on the customer's side (e.g. at a production site). The PLM has limit values to determine whether a peak is too high. If the limits are jeopardised, the PLM delays the tasks of connected machines (here, e.g. SRM). An abstract delay of the tasks of two SRM is displayed in Figure 1.

In this paper, the PLM has to check two different kinds of limits before it can release the task of a machine. The *MAL* is a fixed upper limit for the maximum power. The *MEL* sets the maximum for used power capacity over a period

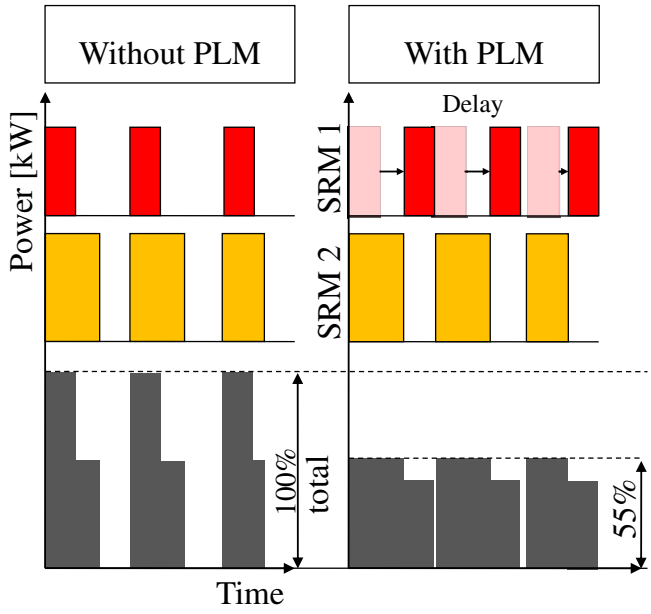

Figure 1. Delay of tasks of SRMs with a power load management (PLM), inspired by Müller et al. (2009).

(15 min). In some cases, it is worth varying the mean power-limit. For example, the mean power-limit can be raised when energy prices decline because of over-production.

2.3 *Energy costs*

Electric energy costs for the industry consist (e.g. in Germany) of the demand charge and the energy charge. With the demand charge, customers pay *inter alia* for the usage of the power grid. It depends on the peak load required over a billing cycle (monthly or annually). With the energy charge, the used energy is paid for, i.e. the consumed amount of energy in the billing period.

2.4 *Literature review*

The literature review is divided into the fields of:

- PLM for production-sites or households
- Energy consumption of AS/RS
- Travel-time models of AS/RS
- Load management for AS/RS

Research in the field of PLM for production-sites aims to reduce the energy consumption peaks and costs. Tasks are postponed to reduce the highest capacity needed (Reinhart and Graßl 2013) or to use more energy in a time period with a lower energy price (Hu, Qin, and Wang 2014). In households, PLM optimises the energy-use of machines (e.g. dryers) to downsize the electric hardware (Bosen and Haepp 2010).

In the international research in the field of AS/RS, only few international papers address the energy efficiency of AS/RS. Thus, there are few papers about modelling the energy-demand of AS/RS (Cárdenas et al. 2009; Ertl and Günthner 2016; Lerher, Edl, and Rosi 2014; Meneghetti, Dal Borgo, and Monti 2015; Meneghetti and Monti 2014; Tappia et al. 2015). Research in the field of AS/RS energy consumption can be divided into three main topics:

- Determining the energy demand in the planning phase
- Reducing the energy demand by hardware optimisation and
- Reducing the energy demand through energy-efficient control and warehouse management strategies.

Research focussing on the field of determining the energy demand during the planning phase aims to find methods to compare the energy demands of different machines. Tappia et al. (2015) developed an analytical model to incorporate

the environmental dimensions of AS/RS and AVS/RS in the assessment of automated warehouses. The results show that AVS/RS need less energy per cycle than AS/RS, but are not always the most economical solution. Ertl and Günthner (2013) developed an analytical method to determine the energy-efficiency of AS/RS for different loads, throughputs and cubatures of the warehouse. To determine the mean energy demand of AS/RS, Ertl and Günthner (2016) developed a meta-model and a simulation model. Besides, Lerher, Edl, and Rosi (2014) developed an energy efficiency model for a mini-load AS/RS to determine the energy demand and the CO_2 emission. This paper builds a good basis for calculating the energy demand of an SRM.

The area of reducing the energy demand by hardware optimisation is distinguished in the optimisation of mechanical or electrical hardware. Lightweight constructions lead to greater energy efficiency (Furmans and Linsel 2011; Günthner et al. 2011). Due to the material and production costs, the payback is too long in both approaches. With DC-link coupling between the axes, energy recuperation units to recover energy, and capacitors as short-term energy storage, energy can be saved (Günthner et al. 2011).

In the field of energy-efficient control strategies, research has shown that reducing the maximum travelling speed of an AS/RS reduces its energy consumption (Meneghetti, Dal Borgo, and Monti 2015; Meneghetti and Monti 2014; Schulz, Monecke, and Zadek 2012). In order to avoid the loss of AS/RS throughput, the speed should only be reduced if the time demand for hoisting is higher than the one for travelling.

In the area of energy-efficient warehouse management strategies, approaches like building energy-efficient double-command cycle couples (Meneghetti, Dal Borgo, and Monti 2015); building and selecting storage zones depending on energy demand (Siegel et al. 2013); selecting storage locations depending on the payload and the resulting energy demand for the task (Meneghetti and Monti 2014; Sommer and Wehking 2013), as well as the use of automated warehouses as energy storage (Voß, Verl, and Schnierle 2014) were explored. All these approaches affect the logistic processes of the warehouse management system, which is avoided in this research.

Much of the research in the field of travel-time analysis determines the travel-time with analytical models. The aim is to calculate the travel-time of the AS/RS (Hwang and Lee 1990; Lerher et al. 2010) or to quantify the impact of I/O positions, dwell-point strategies, the shape of the system, receiving and shipping strategies, storage strategies, order-picking strategies and executing quadruple cycles (Bozer and White 1984; Gu, Goetschalckx, and McGinnis 2007; Xu et al. 2015; Zaerpour, de Koster, and Yu 2013). In the majority of these models, 'Crane acceleration and deceleration are assumed instantaneous and are ignored' (Gagliardi, Renaud, and Ruiz 2012). Only a few take the acceleration and deceleration into account (Hwang and Lee 1990; Lerher et al. 2010). Meller and Mungwattana (2005) used a simulation model to determine the performance and the response time of AS/RS with different dwell-point strategies. Unfortunately, the simulation model is not detailed. Gagliardi, Renaud, and Ruiz (2015) have developed a simulation model to assess the travel-time of an MA-AS/RS with different sequencing approaches. It includes some logistic processes, and acceleration and deceleration is neglected. In addition to the AS/RS, Lerher (2015) developed an analytical model to determine the cycle times for double deep AVS/RS.

Cárdenas et al. (2009) used a PLM to reduce the power peaks of an MA-AS/RS. The method is based on a genetic algorithm approach that calculates the start times of their axes. The paper shows how to determine the start time of two already-known tasks of two SRM, but it does not show how their method applies to realistic tasks which are generally only known shortly before they have to be executed.

The literature review shows that there is no research on the energy demand in all machine states of an MA-AS/RS. In many models, the acceleration and deceleration is neglected or assumed as constant in the calculation of the movements. To represent the behaviour of the SRM precisely, all seven phases of movements (velocity, acceleration and deceleration, as well as jerk) have to be calculated. As Ertl and Günthner (2016) and Lerher, Edl, and Rosi (2014) have suitable approaches for determining the energy demand for the movements of one SRM, these models will be extended in this paper for further investigation.

3. Assumptions

The following assumptions are made for this research:

- The investigated system is a mini-load MA-AS/RS with three aisles and one SRM for each aisle with an LHD for one big or two small totes.
- Each aisle has a double deep storage rack on both sides with 72 columns (x-direction) and 32 rows (y-direction) and one I/O located at the position $X_{IO} = 0\,\text{m}, Y_{IO} = 7\,\text{m}$
- The SRM travels simultaneously in the horizontal and vertical direction and has a DC-link coupling between the hoisting and the travelling drive.

- The SRM operates either single or combined cycles, with a random storage assignment and the remaining strategy as dwell-point strategy.
- The movement trajectories are calculated with speed, acceleration and jerk.

4. Simulation model

After providing the PLM with limits, the PLM delays machine tasks to stay within these limits. These delays have an impact on the material-flow of the automated warehouse. As experiments are very cost-intensive, and because discontinuous processes (e.g. brake controls) as well as the interdependence of single SRM (delaying one SRM will influence the other SRM) make the system too complex for an analytical approach, we opted for a simulative calculation with a simulation model which is capable of dealing with the changing movement paths for the axes, the changing loads and the dependencies between the SRM. Due to the combination of graphical modelling of mathematical formulas and event-driven state machines, we decided to use MatLab® Simulink® as the environment.

The simulation model allows us to calculate the power and energy demand for a task list of an MA-AS/RS. The simulation model, with its inputs and outputs, is displayed in Figure 2. The inputs are:

- A *task list* for every SRM that contains the information on time, machine movement and load (e.g. drive from position X_1/Y_1 to position X_2/Y_2).
- The *layout* defines the number and type (e.g. mini-load system) of the SRM to be simulated.
- The *machine parameters* define all the parameters needed to calculate the movement and energy consumption of the SRM (e.g. travel speed).
- The *PLM parameters* are MEL, MAL and the time period used for calculating the demand charge.

The outputs are:

- *Throughput* of the MA-AS/RS
- *Energy consumption* and *power demand*

The simulation model consists of multiple SRM models and one PLM. The calculations determine the energy demand of an MA-AS/RS and are based on the calculations of Ertl and Günthner (2016). The calculations to simulate the power demand of an MA-AS/RS are described in the following chapters. The PLM model is described in Section 7.

5. Storage and retrieval machine model

To reproduce the behaviour of the SRM, the SRM model consists of the task controller and the inner SRM model (Figure 3). The SRM task controller's objectives are to read the tasks of the task list one by one and to process the needed input data (e.g. travel distance) for the inner SRM model.

The inner SRM model contains the brakes controller, the axes controller and the SRM power model. The axes controller calculates the start times of the axes (Section 5.2) and the brakes controller reproduces the behaviour and controls the states of the brakes (Section 5.3).

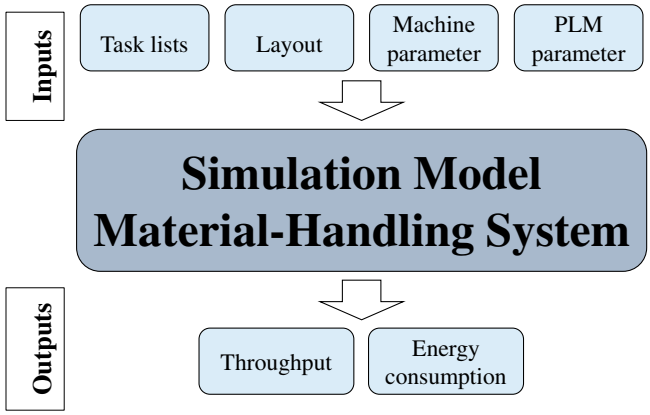

Figure 2. Simulation model with inputs and outputs.

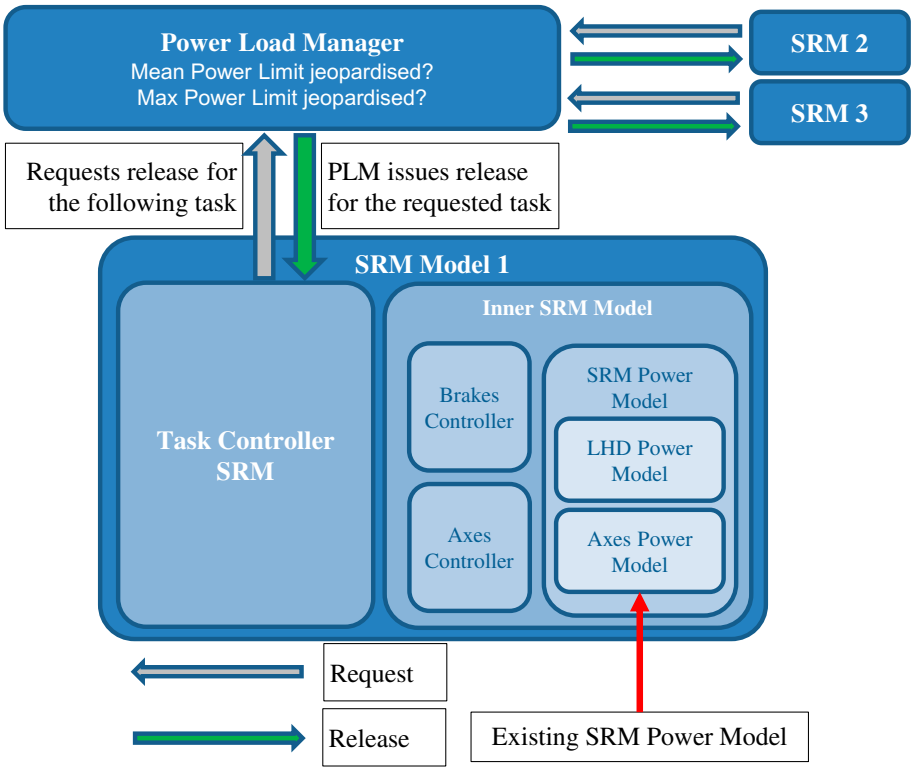

Figure 3. Structure of the simulation model and the SRM model.

The SRM power model contains the LHD and the axes power model. With these power models, the power consumption for the movements of the MA-AS/RS is calculated.

5.1 *SRM task controller*

The task controller of the SRM is implemented as an event-driven system with the modelling tool Stateflow®. It processes the data of the task list and controls the inner SRM model. In addition, it handles the tasks chronologically, ensures that only one task is executed and requests the release of the PLM. For the release request, the task controller calculates the energy prediction for the next task with the travel distance and the load of the task list; the SRM-state machine then sends the release requests with the energy prediction to the PLM. Until the SRM gets a release from the PLM, the task must not be executed. As soon as it gets the release, the inner SRM model is started with the processed data.

5.2 *Axes controller*

Due to the static SRM parameters (e.g. travelling speed, acceleration…) and the varying travel distances for each axis, the time demand for hoisting and travelling is rarely the same. Additionally, the drives work like generators and convert the mechanical energy into electric energy when the torque has the opposite direction to the rotation. Depending on the connection between the axes (Section 6.4), regained energy can be used by another drive, or recovered by varying the start times of the axes.

Take, for example, an SRM movement with a higher time demand for travelling (x-axis) than hoisting (y-axis) and the connection is a DC-link coupling or recuperation: to directly re-use the energy generated by the travelling unit during deceleration, the hoisting process should start as late as possible.

Three special cases are distinguished. The start times of the axes t_{Startx}, t_{Starty} are calculated with the time demands for travelling t_x and for hoisting t_y, and the distances for travelling s_x and for hoisting s_y using the following formulae:

Case 1: $(t_y > t_x \wedge s_y < 0)$

$$t_{Startx} = t_y - t_x \tag{3}$$

$$t_{Starty} = 0 \tag{4}$$

Case 2: $(t_y < t_x \wedge s_y > 0)$

$$t_{Startx} = 0 \tag{5}$$

$$t_{Starty} = t_x - t_y \tag{6}$$

In all other cases, the hoisting and the travelling movements start at the same time.

5.3 *Brakes controller*

The controller for the brakes is important for the processing of the tasks and for the power demand of the SRM during the idle state and during the LHD tasks. As the drive has to be magnetised and has to keep the position of the SRM or the LHD, the power demand of an SRM rises when the brakes are released. In addition, it takes time to open the brakes, which delays the start time of the movement.

6. SRM power model

The SRM power model contains mainly the LHD power model and the axis power model. In addition, it calculates the energy consumption of the on-board cabinet.

In the following, the drive trains for travelling and hoisting and their connection, as well as the LHD power model, are described. The consumption of the on-board cabinet is measured on a test system and implemented in this model as a constant.

The SRM has two main drive trains, one for travelling and one for hoisting. The drive trains deliver power for the movements of the SRM. For the SRM, they convert the electric power into mechanical power. Figure 4 illustrates the energy supply of an SRM (drive wheel (DW), belt drive (BD), gearbox (GB), drive unit (DU), travel unit (TU) and hoisting unit (HU)). To calculate the power and energy demand, the following calculation steps are needed:

(1) Movement trajectory for both movements
(2) Power demand of both drives

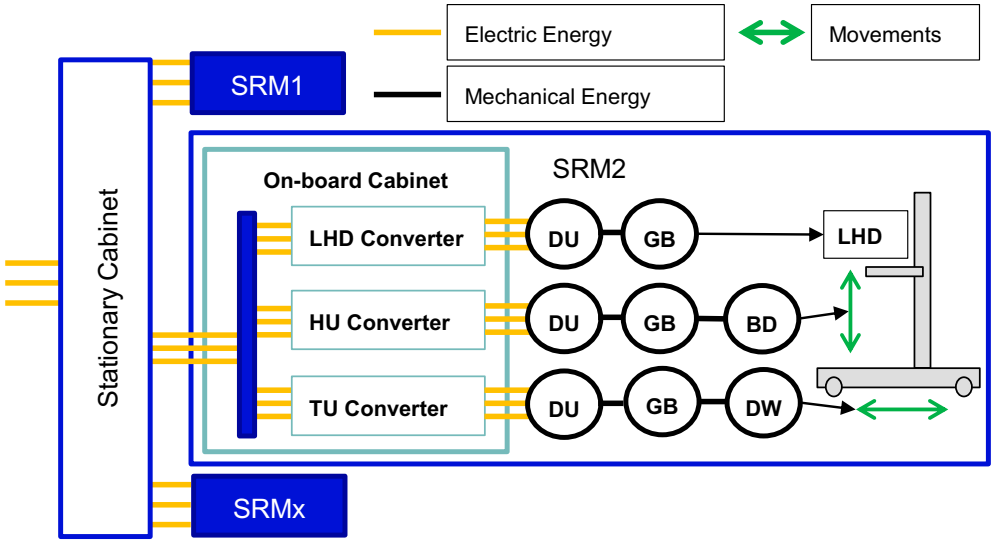

Figure 4. Energy supply of a SRM.

(3) Power demand of the frequency converters
(4) Power demand depending on the connection between the axes
(5) The LHD power demand
(6) On-board cabinet and stationary cabinet power demand

All these steps are needed to calculate the energy demand and are described in detail in the following sections.

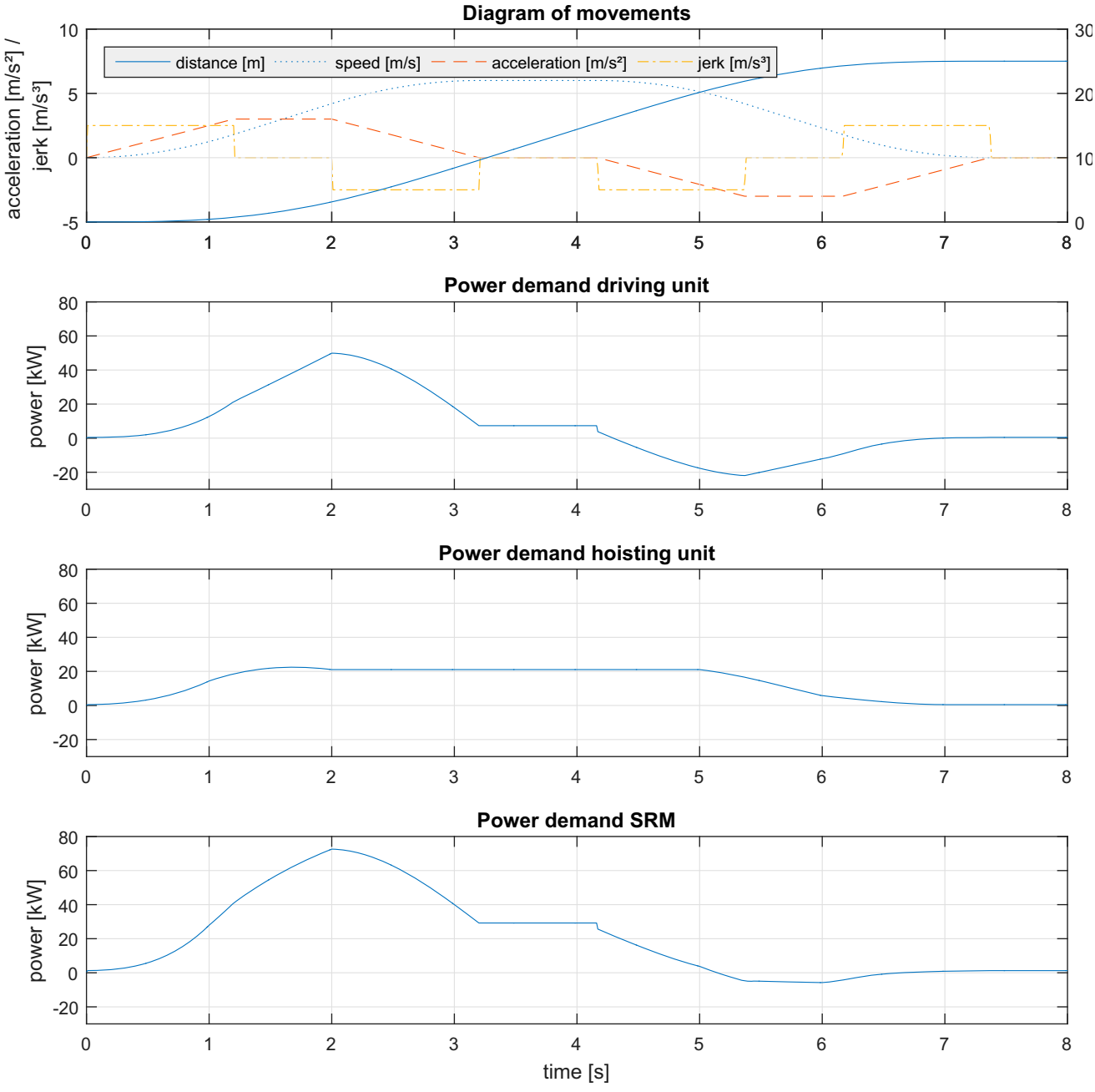

Figure 5. Movement trajectory and power demand diagrams of a SRM.

6.1 *Movement trajectory for both movements*

The linear movement of the machine along the x and y-axes is divided into seven phases. The trajectory of a movement with the seven phases in which the maximum speed is reached is shown in Figure 5. The phases are:

(1) Jerk-phase (increasing acceleration)
(2) Constant acceleration phase
(3) Jerk-phase (declining acceleration)
(4) Constant speed phase
(5) Jerk-phase (increasing deceleration)
(6) Constant deceleration phase
(7) Jerk-phase (declining deceleration)

Depending on the travel distance of the movement and the dynamic parameters (speed, acceleration, jerk), neither the maximum speed, nor the maximum acceleration can be reached. The trajectory calculation is based on the work of Ertl and Günthner (2016).

6.2 *Power demand for both drives*

The calculation of the power demand of both drives is based on the model of Ertl and Günthner (2016). Generally, asynchronous drives or asynchronous servo-drives are used for SRM. The power demand of the travelling unit drive is displayed in Figure 5. The diagram of the power demand of the travelling unit shows the three phases of the power demand of a travelling movement. The acceleration, the constant speed and the deceleration phase. To calculate the torque of the travelling drive M_{Dx} during a movement of the SRM acceleration *axe*, the mass of the SRM including the load m_{SRM}, the normal force on the drive wheel F_{NDW}, the rolling resistance coefficient f_{RRx}, the velocity-dependent rolling resistance F_{RRvdx}, the radius of the drive wheel r_{DW}, the gear ratio i_{GBx}, the acceleration-dependent efficiency factors of the drive wheel η^*_{DW} and the gearbox η^*_{GBx} and the moments of inertia of the drive wheel J_{DW}, the gear box J_{GBx} and the drive J_{Dx} are needed:

$$M_{Dx}(t) = \frac{(a_x(t)m_{SRM} + F_{NDW}f_{RRx} + F_{RRvdx}(t))r_{DW}}{\eta^*_{DW}\eta^*_{GBx}i_{GBx}} + \frac{J_{DW}a_x(t)}{r_{DW}i_{GBx}\eta^*_{GBx}} + \frac{a_x(t)i_{GBx}}{r_{DW}}(J_{GBx} + J_{Dx}) \tag{7}$$

With the torque M_{Dx} and the angular speed of the drive ω_{Dx}, the power demand of the travelling unit drive P_{Dx} is calculated:

$$P_{Dx}(t) = \frac{M_{Dx}(t)\omega_{Dx}(t)}{\eta^*_{Dx}} \tag{8}$$

The acceleration-dependent efficiency factors for the gearbox η^*_{GBx}, the drive wheel η^*_{DW} and the drive η^*_{Dx} of the travelling unit depend on the acceleration of the drive unit and are calculated with the efficiency factors of the gear box η_{GBx}, the drive wheel η_{DW} and the drive η_{Dx} and the efficiency factor reduction of the gearbox during breaking η_{GBredx}:

$$\eta^*_{GBx}(a_x(t)) = \begin{cases} \eta_{GBx}, & a_x \geq 0 \\ \frac{1}{\eta_{GBx} - \eta_{GBredx}}, & a_x < 0 \end{cases} \tag{9}$$

$$\eta^*_{DW}(a_x(t)) = \begin{cases} \eta_{DW}, & a_x \geq 0 \\ \frac{1}{\eta_{DW}}, & a_x < 0 \end{cases} \tag{10}$$

$$\eta^*_{Dx}(a_x(t)) = \begin{cases} \eta_{Dx}, & a_x \geq 0 \\ \frac{1}{\eta_{Dx}}, & a_x < 0 \end{cases} \tag{11}$$

To calculate the torque of the hoisting drive M_{Dy} during the movement of the SRM, the speed v_y, the acceleration a_y, the mass of the LHD including the load m_{LHD}, the rolling resistant force F_{RRy}, the radius of the driven toothed-belt disc

r_{BD}, the gear ratio i_{GBy}, the direction-dependent efficiency factors of the belt drive η^*_{BD} and the gearbox η^*_{GBy}, the moments of inertia of the belt drive J_{BD}, the gear box J_{GBy} and the drive J_{Dy} and the direction factor d_y are needed:

$$M_{Dy}(t) = \left(\frac{\left(m_{LHD} a_y(t) + F_{RRy}(t)\right) r_{BD}}{\eta^*_{BD} \eta^*_{GBy} i_{GBy}} + \frac{J_{BD} a_y(t)}{r_{BD} i_{GBy} \eta^*_{GBy}} + \frac{\left(J_{GBy} + J_{Dy}\right) a_y(t) i_{GBy}}{r_{BD}} \right) d_y + \frac{m_{LHD} r_{BD} g}{\eta^*_{BD} \eta^*_{GBy} i_{GBy}} \tag{12}$$

$$d_y = \begin{cases} 1, & v_y(t) > 0 \\ -1, & v_y(t) \leq 0 \end{cases} \tag{13}$$

For the calculation of the rolling resistant force F_{RRy}, the normal force F_{NRy} on the rollers of the LHD, the rolling resistance coefficient f_{RRy} and the velocity-dependent rolling resistance F_{RRvdy} are needed:

$$F_{RRy}(t) = \begin{cases} F_{NRy} f_{RRy} + F_{RRvdy}(t), & v_y(t) \neq 0 \\ -F_{NRy} f_{RRy} - F_{RRvdy}(t), & v_y(t) = 0 \end{cases} \tag{14}$$

The direction-dependent efficiency factors for the gearbox η^*_{GBy}, the drive wheel η^*_{BD} and the drive η^*_{Dy} of the hoisting unit are calculated with the hoisting speed v_y (upwards positive, downwards negative), the efficiency factors of the gear box η_{GBy}, the belt drive η_{BD} and the drive η_{Dy} and the efficiency factor reduction of the gearbox during breaking η_{GBredy}:

$$\eta^*_{GBy}(v_y(t)) = \begin{cases} \eta_{GBy}, & v_y > 0 \\ \frac{1}{\eta_{GBy}}, & v_y = 0 \\ \frac{1}{\eta_{GBy} - \eta_{GBredy}}, & v_y < 0 \end{cases} \tag{15}$$

$$\eta^*_{BD}\left(v_y(t)\right) = \begin{cases} \eta_{BD}, & v_y > 0 \\ \frac{1}{\eta_{BD}}, & v_y \leq 0 \end{cases} \tag{16}$$

$$\eta^*_{Dy}(v_y(t)) = \begin{cases} \eta_{Dy}, & v_y \geq 0 \\ \frac{1}{\eta_{Dy}}, & v_y < 0 \end{cases} \tag{17}$$

The hoisting drive's power P_{Dy} is calculated as follows:

$$P_{Dy}(t) = \frac{\left(a_y(t) m_{LHD} + F_{RRy}(t)\right) \left|v_y(t)\right|}{\eta^*_{BD} \eta^*_{GBy} \eta^*_{Dy}} + \frac{J_{BD} a_y(t) \left|v_y(t)\right|}{r^2_{BD} \eta^*_{GBy} \eta^*_{Dy}} + \frac{\left|v_y(t)\right| a_y(t) i^2_{GBy}}{r^2_y \eta^*_{Dy}} \left(J_{GBy} + J_{Dy}\right) + \frac{m_{LHD} v_y(t) g}{\eta^*_{BD} \eta^*_{GBy} \eta^*_{Dy}} \tag{18}$$

In addition to the existing model, the drive current I_{Di} for asynchronous drives (following $i = x$ for travelling unit; $i = y$ for hoisting unit) is calculated with the drive's nominal torque M_{DNi}, nominal current I_{NDi}, magnetisation current I_{DMi} and efficiency factor η^*_{Di} (Riese and Fräger 2008):

$$I_{Di}(t) = \frac{\sqrt{\frac{M^2_{Di}(t)}{M^2_{DNi}} \left(I^2_{DNi} - I^2_{DMi}\right) + I_{DMi}}}{\eta^*_{Di}} \tag{19}$$

6.3 *Power demand of the frequency converters*

To calculate the power for the frequency converter P_{FCi} (following $i = x$ for travelling unit; $i = y$ for hoisting unit), the power of the connected drive P_{Di} and the power loss of the frequency converter P_{FCLi} are needed. The power loss is calculated with the frequency converter's nominal power loss P_{FCLNi}, the power loss when disabled P_{FCLci}, the nominal current I_{FCNi} and the current of the connected drive I_{Di} (Riese and Fräger 2008):

$$P_{FCi}(t) = P_{Di}(t) + P_{FCLi}(t) \tag{20}$$

$$P_{FCLi}(t) = \begin{cases} P_{FCLci} + (P_{FCLNi} - P_{FCLci})\frac{I_{Di}(t)}{I_{FCNi}}, I_{Di} \geq 0A \\ P_{FCLci}, I_{Di} < 0A \end{cases} \quad (21)$$

If the brake for the drive is closed, the torque M_{Dy} and the current I_{Dy} of the hoisting drive are zero.

6.4 *Connection between axes*

Depending on the connection between the frequency converters of the x and y-axes, the energy can or cannot be recuperated. The main connection types are DC-link coupling and energy recovery. *DC-link coupling* means that the DC circuits of the AS/RS frequency converters are connected. That way, the regenerated power of one axis can be transferred to the other axis. The power for the SRM axes $P_{SRMAxes}$ is calculated with the power demand of both frequency converters P_{FCx} and P_{FCy}:

$$P_{SRMAxes}(t) = \begin{cases} P_{FCx}(t) + P_{FCy}(t), P_{FCx}(t) + P_{FCy}(t) \geq P_{FCLcx} + P_{FCLcy} \\ P_{FCLcx} + P_{FCLcy}, P_{FCx}(t) + P_{FCy}(t) < P_{FCLcx} + P_{FCLcy} \end{cases} \quad (22)$$

If the AS/RS has a system for *energy recovery* installed, the regenerated power can be transferred between the axes and then back to the supplying electricity grid. The energy recovery units suffer a power loss P_{RUL} depending on the load. To calculate the loss, the energy recovery's nominal power P_{RUN}, nominal power loss P_{RULN} and power loss when disabled P_{RULc} is needed. There is an efficiency factor for recovering the energy η_{RC}. The power for the SRM axes $P_{SRMAxes}$ is:

$$P_{SRMAxes}(t) = \begin{cases} \left(P_{FCx}(t) + P_{FCy}(t) + P_{RUL}(t)\right)\eta_{RC}, P_{FCx}(t) + P_{FCy}(t) + P_{RUL}(t) < 0 \\ P_{FCx}(t) + P_{FCy}(t) + P_{RUL}(t), P_{FCx}(t) + P_{FCy}(t) + P_{RUL}(t) \geq 0 \end{cases} \quad (23)$$

$$P_{RUL}(t) = P_{RULc} + (P_{RULN} - P_{RULc})\frac{|P_{SRMAxes}(t)|}{P_{RUN}} \quad (24)$$

6.5 *LHD power model*

The LHD power model simulates the power demand of the LHD. The power demand of an SRM during the LHD cycle is a combination of the power demand for holding the position with the hoisting unit, and the power demand for the movements of the LHD. The power demand for the hoisting unit in the simulation model is achieved by opening its brake during the cycle. The power demand of the LHD is read from a file with a representative measured power demand (e.g. single-deep cycle of a Box Gripper).

6.6 *On-board cabinet and the stationary cabinet power demand*

The on-board cabinet distributes the electrical energy to the drives and the LHD and has some other electrical components (e.g. safety components) installed. The power demand of these components is simplified and reduced to one parameter, the power demand of the on-board cabinet P_{OC}. Thus, with the power of the SRM axes $P_{SRMaxes}$ and the power of the LHD P_{LHD}, the power demand of the SRM $P_{SRM}(t)$ is:

$$P_{SRM}(t) = P_{SRMAxes}(t) + P_{LHD}(t) + P_{OC} \quad (25)$$

The stationary cabinet distributes the electrical energy to the connected SRM and contains components for the energy distribution, the control of the SRM (e.g. IT components) and the energy measurement. The power demand of these components is reduced to the constant power demand of the stationary cabinet P_{SCc}. The power demand of the stationary cabinet P_{SC} needed to supply the connected SRM P_{SRMi} is calculated as follows:

$$P_{SC}(t) = P_{SCc} + \sum_{i=1}^{n} P_{SRMi}(t) \quad (26)$$

7. PLM model

The objective of the PLM is to make sure that the energy consumption of the AS/RS remains under the set limits. To achieve this, it checks whether the requested task will violate the limits. In case of a violation, the PLM delays the task to prevent the violation of the limits. To check whether the limit is jeopardised, the PLM needs the energy demand of the already-released tasks, the so-called 'power demand prediction'.

As soon as the PLM receives a request from an SRM, it has to check both limits regarding their violation. To check the limits, the PLM calculates the expectable power demand by adding the pre-calculated power demand of the task to the power demand prediction.

For the *mean power check*, the PLM checks whether the mean of the expected power demand for this period is higher than the MEL. If there is no violation, the check is passed.

For the *maximum power check,* the maximum of the expected power demand is checked against the MAL. If there is no violation, this test is passed.

If any of the checks are not passed, the task is delayed and both checks are repeated in the next time-step. The simplified communication between the SRM and the PLM is illustrated in Figure 3.

If both checks are passed, the power demand prediction is updated with the pre-calculated demand of the released task. The expected power demand is therefore saved as the new prediction.

The PLM is modelled as a state machine with inputs for every SRM. As a state machine, the PLM is an event-driven programme and checks the request when the request event occurs.

8. Calibration and validation of the model

For the calibration and validation of the model, the simulation results are compared with the measured data of a real system. This step is used to show that the simulation model represents the respective system and can be used to study the behaviour of the MA-AS/RS.

The calibration and validation of the simulation model is handled stepwise. These steps are:

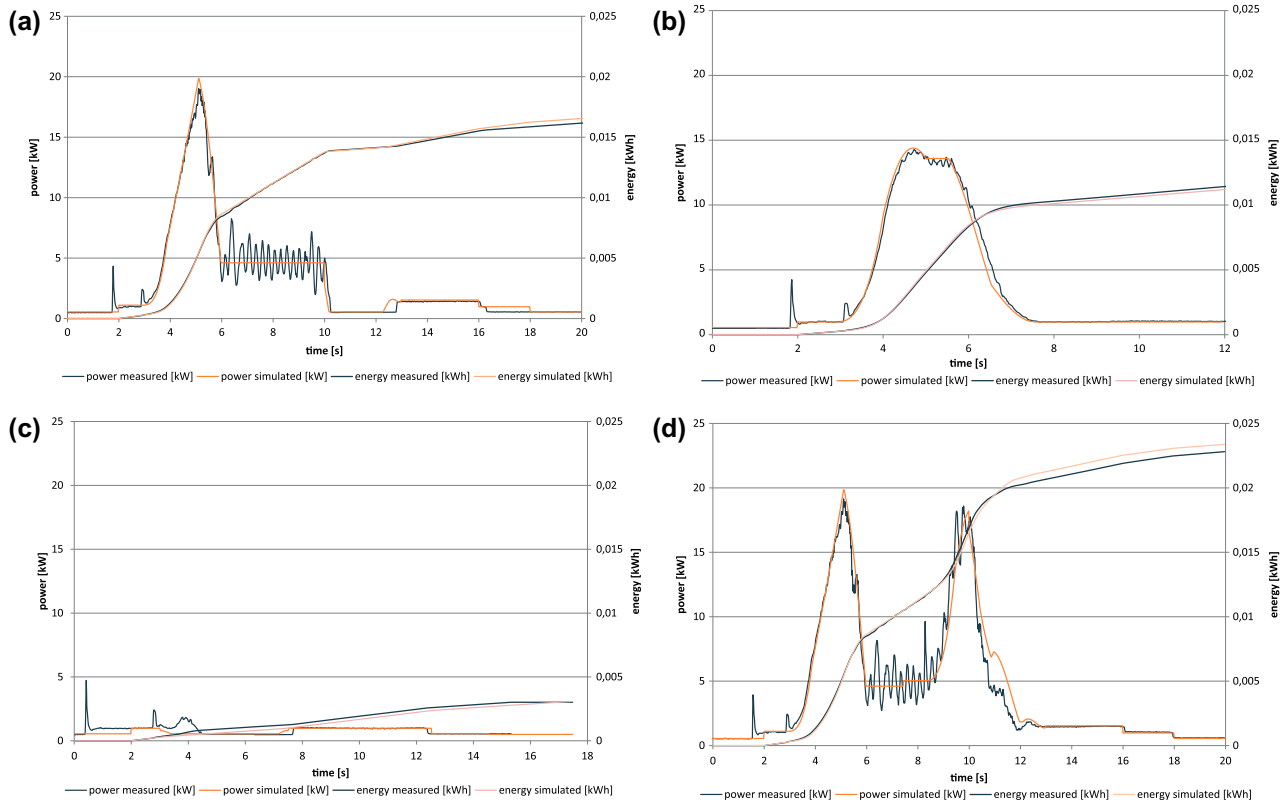

Figure 6. (a) $s_x = 28\,\text{m}; s_y = 0.01\,\text{m}$. (b) $s_x = 0\,\text{m}; s_y = 7.56\,\text{m}$. (c) $s_x = 0\,\text{m}; s_y = -7.56\,\text{m}$. (d) $s_x = 28\,\text{m}; s_y = 7.59\,\text{m}$.

Table 1. Deviation between measured and simulated energy demand of the AS/RS for one week.

	Measured	100% load	50% load	0% load
Mean deviation (kW)	–	0.059	0.037	0.015
Max deviation (kW)	–	0.372	0.309	0.247
Min deviation (kW)	–	−0.134	−0.165	−0.196
Mean deviation (%)	–	2.45%	2.13%	1.91%
Max deviation (%)	–	7.26%	7.07%	7.07%
Min deviation (%)	–	0.01%	0.00%	0.00%
Total energy demand (kWh)	411.82	418.58	416.06	413.57
Total energy deviation (kWh)	–	6.760	4.233	1.748
Total energy deviation (%)		1.64%	1.03%	0.42%

(1) Calibration of torque and power demand of the axes (Figure 6(a)–(c)
(2) Validation of the SRM for combined movements (Figure 6(d))
(3) Validation of the power of the MA-AS/RS over a longer period of time

In this step, the simulation model is validated. First of all, the energy demands of the SRM and then of the MA-AS/RS are validated. The energy demand of the SRM is validated with the measured energy demands of the movements of a real SRM, as shown in Figure 6. The results show that there is a high correlation between the simulation and the measurement.

To validate the energy demand of the MA-AS/RS, a power measurement system installed in the cabinet measures the used energy of the three SRM every 15 min. In addition, the movements of the SRM during the measurement are recorded in files. With the information of the SRM and their movements, the simulation is executed. The recorded movements of the SRM are distributed over the entire length and height of the rack. The average material flow of this AS/RS over the week is 35 storages/hour, 36 retrievals/hour and 8 relocations/hour.

The simulation results are compared with the measured energy demand. The results (Table 1) show that the simulation model nearly delivers the measured mean power in 15 min.

9. Simulation

In this paper, a mini-load system with three identical SRM is simulated. These SRM are connected to the same stationary cabinet. A part of the recorded task list of the real system containing mixed single- and double-cycles is used.

To determine the throughput of the MA-AS/RS, the simulation model reports, after each simulation, how many storages and retrievals each SRM has completed. With these data, the average throughput for one SRM is calculated. The MAL and the MEL are reduced stepwise.

In the first step, the full system throughput is simulated. Every SRM therefore executes its tasks without any idle time in between. As the results represent the maximum system throughput, they form the reference for all further simulations in this paper. The results for the throughput for high dynamic parameters (HDP; $v_x = 6\,\frac{m}{s}; a_x = 3\,\frac{m}{s^2}; v_y = 3\,\frac{m}{s}; a_y = 3\,\frac{m}{s^2}$) and low dynamic parameters (LDP; $v_x = 4\,\frac{m}{s}; a_x = 1.9\,\frac{m}{s^2}; v_y = 3\,\frac{m}{s}; a_y = 3\,\frac{m}{s^2}$) are displayed in the Figures 7 and 8 as ‘HDP w/o PLM’ and ‘LDP w/o PLM’.

The simulation results are illustrated in the Figures 7 and 8. Figure 7 shows the impact of the MAL on the throughput of the system with high dynamic parameters and low dynamic parameters. As mentioned before, the horizontal lines, ‘HDP w/o PLM’ and ‘LDP w/o PLM’, show the throughput of the system with deactivated PLM. The markers on the lines with PLM-activated represent the result of a simulation run. The MEL is reduced stepwise. In the ‘Worst-Case’, in which the three SRM have the maximum power-peak at the same time, the power demand of the high dynamic parameters is 117 kW, and the one of the low dynamic parameters is 93 kW. The differences between the maximum of the ‘HDP with PLM’ line and the ‘HDP w/o PLM’, and between the maximum of the ‘LDP with PLM’ line and the ‘LDP w/o PLM’ show the loss of throughput due to the activation of the PLM. With high dynamic parameters and low dynamic parameters, the loss of throughput through the activation of the PLM is 4% for sufficiently large MAL.

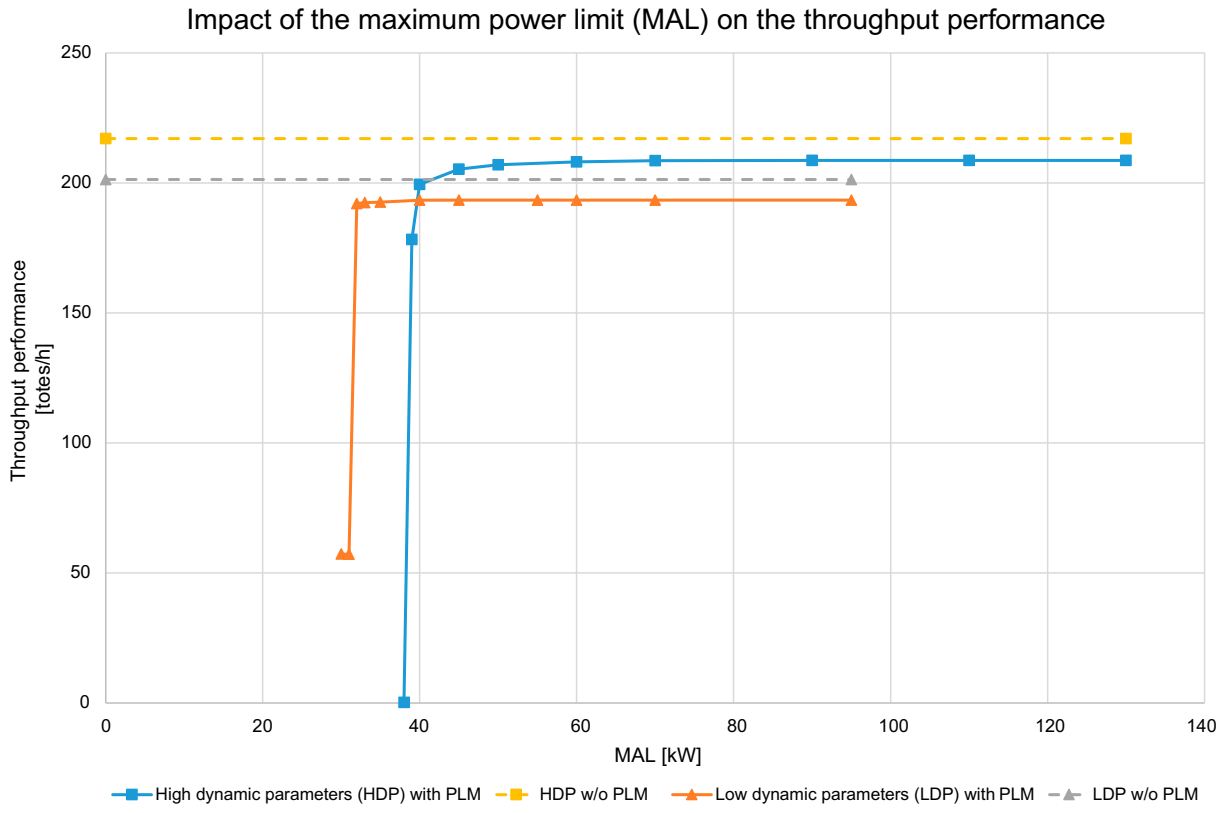

Figure 7. Throughput performance without PLM and with PLM and maximum power limits (MAL); Mean power limit: *MEL* = 1000 kW.

As can be seen, the PLM has little impact on the throughput of the MA-AS/RS by reducing the MAL to 50 kW (high dynamic parameters) or to 34 kW (low dynamic parameters). Lower limits significantly reduce the throughput. With an MAL of 38 kW (high dynamic parameters) or 31 kW (low dynamic parameters), the system stops at a specific time. This is due to the fact that the power demand of the next task has a higher power demand than the MAL and thus never gets a release from the PLM.

The impact of the MEL on the throughput of the AS/RS is illustrated in Figure 8. The reduction of the throughput is nearly proportional to the reduction of the MEL. Even with an MEL of 2 kW, the system performs tasks.

In the figure, the line of the low dynamic parameters is above the line of the high dynamic parameters. This shows that, with the same MEL, the AS/RS with low dynamic parameters achieves a higher throughput than the one with high dynamic parameters. The throughput of the system with the low dynamic parameters at an MEL of e.g. 8 kW is $137\,\frac{\text{movements}}{\text{h}}$ and the one with the high dynamic parameters is $108\,\frac{\text{movements}}{\text{h}}$.

The used strategy of the PLM stops the SRM tasks by reaching the MEL. This means, for example, that if the MEL is jeopardised after 2 min in a period of 15 min, the SRM stops working for the remainder of the period.

The results cannot be compared with those of other studies, because there is no other research in this field. As it happens, through the activation of the PLM, there is a loss of throughput of 4%. This loss is mainly because of the simulation steps needed to get the release and the simulation step-size. In five hours, each SRM processes about 3300 tasks which leads, with one step (0.1s) needed for the release, to a total delay of 990s.

The small impact of the MAL was expected, because the high power-peaks of one SRM occur rarely and for a short time. There is a small chance that the peaks of two or more SRM could superimpose.

The MEL results show that, at the same limit with the low dynamic parameters, a higher throughput can be reached; this is because, with high dynamic parameters, the energy loss of the SRM (e.g. friction, heat…) is higher. This result shows that the dynamic parameters should preferably be reduced when the MEL is lowered.

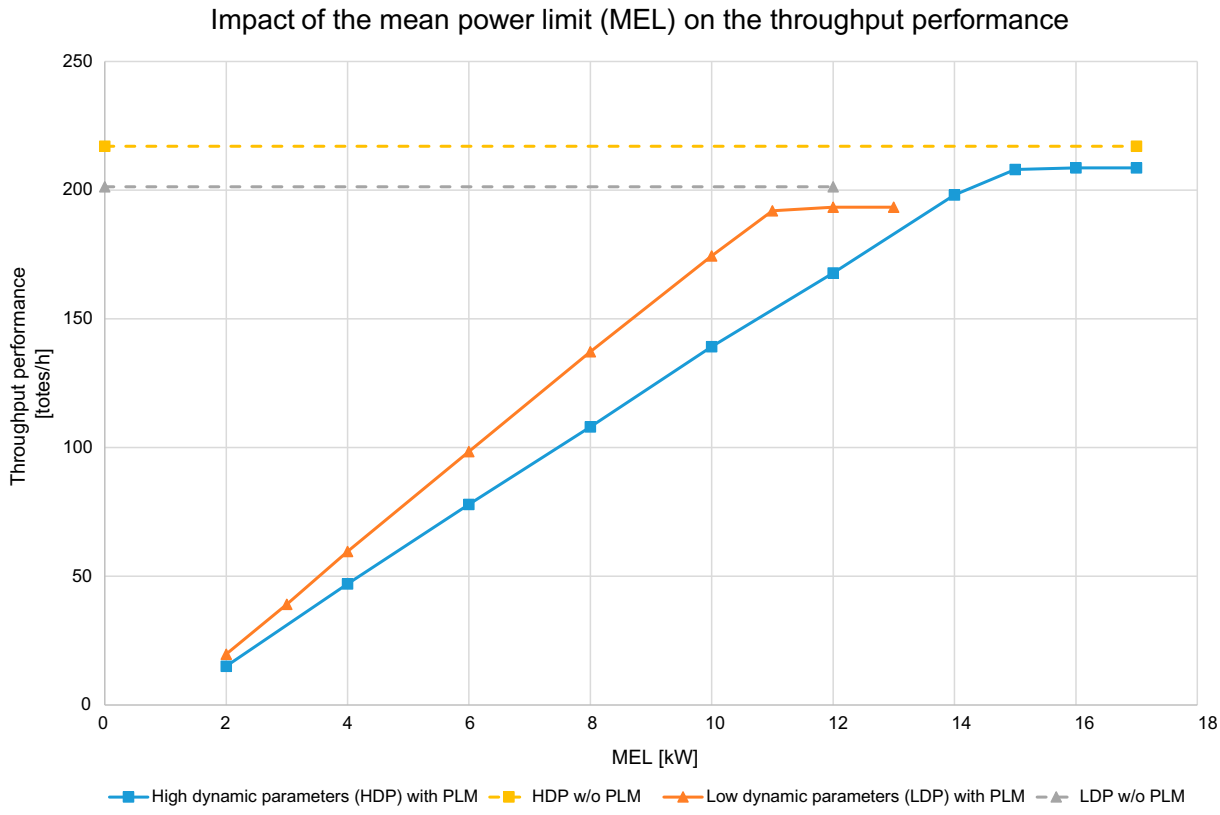

Figure 8. Throughput performance without PLM and with PLM and mean power limits (MEL); Maximum power limit: *MAL* = 1000 kW.

10. Conclusion

This paper provides an answer concerning the influence of a PLM on the throughput of an MA-AS/RS. The PLM ensures that the mean power and the maximum power-limits are not exceeded. To do so, it postpones tasks in case of a violation of any limit.

In this study, a simulation model was built to identify the impact of the PLM on the throughput. It simulates the electrical energy demand of an MA-AS/RS. For that purpose, the layout of the system, the SRM parameters, a task list and the limits for the PLM were needed.

The results of the simulation show that the PLM has an impact on the throughput of an MA-AS/RS. The release request for every task of the SRM needs time, which reduces the throughput in the simulation model by about 4%. To release the task, the PLM needs at least one simulation step. Nevertheless, with PLM, the maximum mean power in a period, and the maximum used power of an MA-AS/RS, can be controlled. Using an MEL, the throughput of a system with the same dynamic parameters (maximum speed, acceleration and jerk) is proportionally reduced. As the energy demand of the tasks does not change, the mean energy demand has to be reduced by postponing the tasks. With the described strategy for the PLM, it stops all the SRM for the remainder of the period when the MEL of that period is reached. An alternative approach would be to reduce the dynamic parameters of the MA-AS/RS for the period. This would reduce the power demand of the task, and thereby the mean power demand of the system, without stopping the system until the next period starts. The results show that the MEL can only be reduced with a throughput loss.

The results of the MAL variation show that limiting the maximum power-peak by 50% only slightly reduces the throughput of the system. The high power demand of the SRM occurs when the acceleration of the travelling unit and the lifting of the hoisting unit are contemporaneous. The probability that multiple SRM are lifting with a high power demand and full workload is very low. If the maximum power-limit is set to a level lower than the maximum power needed for a task of one SRM, the system stops and is blocked as soon as a task with this power demand is on the task list.

With these results, it is important that the MAL is higher than the maximum power needed by one SRM. If operators accept a throughput loss of 5%, PLM is an appropriate tool to limit the maximum electrical power used by their system and to reduce its hardware costs.

These results are valid for this use case and would have to be checked for other use cases. It is, therefore, important to find out how the results are influenced by the task lists, the dynamic parameters of the SRM, the number of SRM and the kind of MA-AS/RS (mini-load system or high-bay warehouse).

Disclosure statement

No potential conflict of interest was reported by the authors.

ORCID


Paul Hahn-Woernle http://orcid.org/0000-0002-5580-5186

References

Bosen, Peter, and Claudia Haepp. 2010. "Domestic Appliance Comprising a Communication Unit, System of Appliances and Method for Operating a Domestic Appliance." US2012124401 (A1). US201013384246 20100708, filed July 8, 2010, and issued May 17, 2012.

Bozer, Yavuz A., and John A. White. 1984. "Travel-Time Models for Automated Storage/Retrieval Systems." *IIE Transactions* 16 (4): 329–338. doi:10.1080/07408178408975252.

Cárdenas, Juan Jose A., Antonio E. Garcia, Jose Luis M. Romeral, and Fabio R. Andrade. 2009. "A Genetic Algorithm Approach to Optimization of Power Peaks in an Automated Warehouse." 35th Annual Conference of IEEE Industrial Electronics(IECON), Porto, 3297–3302.

Ertl, Rainer, and Willibald A. Günthner. 2013. "Schnell Zu Aussagekräftigen Werten Gelangen – Teil 1: Analytische Berechnung Des Mittleren Energiebedarfs Von Regalbediengeräten Mit Energierückspeisung." *Fördern und Heben* 6: 12–14.

Ertl, Rainer, and Willibald A. Günthner. 2016. "Meta-Model for Calculating the Mean Energy Demand of Automated Storage and Retrieval Systems." *Logistics Journal* 1–11. doi:10.2195/lj_NotRev_ertl_en_201602_01.

FEM 9.851. 2003. *Leistungsnachweis Für Regalbediengeräte – Spielzeiten*. No. 9.851. Paris: Federation Europeenne de la Manutention.

Furmans, Kai, and Peter Linsel. 2011. "Leichtbau Bei Unstetigförderern Durch Einsatz Moderner Werkstoffe." *Logistics Journal: Proceedings* 7 (1): 1–12. doi:10.2195/LJ_proc_furmans_de_201108_01.

Gagliardi, Jean-Philippe, Jacques Renaud, and Angel Ruiz. 2012. "Models for Automated Storage and Retrieval Systems: A Literature Review." *International Journal of Production Research* 50 (24): 7110–7125. doi:10.1080/00207543.2011.633234.

Gagliardi, Jean-Philippe, Jacques Renaud, and Angel Ruiz. 2015. "Sequencing Approaches for Multiple-Aisle Automated Storage and Retrieval Systems." *International Journal of Production Research* 53 (19): 5873–5883. doi:10.1080/00207543.2015.1012600.

Gu, Jinxiang, Marc Goetschalckx, and Leon F. McGinnis. 2007. "Research on Warehouse Operation: A Comprehensive Review." *European Journal of Operational Research* 177 (1): 1–21. doi:10.1016/j.ejor.2006.02.025.

Günthner, Willibald A., Michael Schipplick, Rainer Ertl, and Paul Hahn-Woernle. 2011. "Wettbewerbsfaktor energieeffizienz: Simulationsmodell für entwicklung und betrieb von automatischen regalbediengeräten." *Fördern und Heben* 4: 2–5.

Hu, Fei, Jianrong Qin, and Jiacun Wang. 2014. "Electrical Load Schedule Optimization for Manufacturing Plants." Proceedings of the 11th IEEE International Conference on Networking, Sensing and Control (ICNSC), Miami, FL, 7–12.

Hwang, Hark, and Seong Beak Lee. 1990. "Travel-Time Models Considering the Operating Characteristics of the Storage and Retrieval Machine." *International Journal of Production Research* 28 (10): 1779–1789. doi:10.1080/00207549008942833.

Lerher, Tone. 2015. "Travel Time Model for Double-Deep Shuttle-Based Storage and Retrieval Systems." *International Journal of Production Research* 54 (9): 2519–2540. doi:10.1080/00207543.2015.1061717.

Lerher, Tone, Matjaz Sraml, Iztok Potrc, and Tomaz Tollazzi. 2010. "Travel Time Models for Double-Deep Automated Storage and Retrieval Systems." *International Journal of Production Research* 48 (11): 3151–3172. doi:10.1080/00207540902796008.

Lerher, Tone, Milan Edl, and Bojan Rosi. 2014. "Energy Efficiency Model for the Mini-Load Automated Storage and Retrieval Systems." *International Journal of Advanced Manufacturing Technology* 70 (1–4): 97–115. doi:10.1007/s00170-013-5253-x.

Meller, Russell D., and Anan Mungwattana. 2005. "AS/RS Dwell-Point Strategy Selection at High System Utilization: A Simulation Study to Investigate the Magnitude of the Benefit." *International Journal of Production Research* 43 (24): 5217–5227. doi:10.1080/00207540500215617.

Meneghetti, Antonella, and Luca Monti. 2014. "Multiple-Weight Unit Load Storage Assignment Strategies for Energy-Efficient Automated Warehouses." *International Journal of Logistics Research and Applications* 17 (4): 304–322. doi:10.1080/13675567.2013.861896.

Meneghetti, Antonella, Eleonora Dal Borgo, and Luca Monti. 2015. "Rack Shape and Energy Efficient Operations in Automated Storage and Retrieval Systems." *International Journal of Production Research* 53 (23): 7090–7103. doi:10.1080/00207543.2015.1008107.

Müller, Egon, Jörg Engelmann, Thomas Löffler, and Jörg Strauch. 2009. *Energieeffiziente Fabriken planen und Betreiben*. 1st ed. Berlin-Heidelberg: Springer-Verlag.

Reinhart, Gunther, and Markus Graßl. 2013. "Energieflexible Fabriken: Massnahmen Zur Steuerung Des Energiebedarfs Von Fabriken." *VDI-Expertenforum Energiemanagement*. Accessed September 2, 2015. https://m.vdi.de/uploads/media/Grassl_1_.pdf

Riese, Stephan, and Carsten Fräger. 2008. *Antriebslösungen: Formeln, Auslegung und Tabellen*. 1st ed. Hameln: CW Niemeyer. Accessed July 1, 2016.

Schulz, Robert, Jörg Monecke, and Hartmut Zadek. 2012. "Der Einfluss Kinematischer Parameter auf den Energiebedarf eines Regalbediengerätes." *Logistics Journal Proceedings* 1–10. doi:10.2195/lj_Proc_schulz_de_201210_01.

Siegel, Armin, Robert Schulz, Karsten Turek, Thorsten Schmidt, and Hartmut Zadek. 2013. "Modeling the Energy Need of Storage and Retrieval Vehicles and Different Storage Operating Strategies for the Reduction of the Energy Need." [Regalbediengeräten und Verschiedener Lagerbetriebsstrategien zur Reduzierung des Energiebedarfs.] *Logistics Journal* 2013 (10): 1–18. doi:10.2195/lj_Proc_siegel_de_201310_01.

Sommer, Tobias, and Karl-Heinz Wehking. 2013. "Energy Efficient Storage Location Assignment in Automated Storage and Retrieval Systems (aS/RS)." [Energieeffiziente Lagerplatzzuordnung in Hochregallagern.] *Logistics Journal* 2013 (10): 1–10. doi:10.2195/lj_Proc_sommer_de_201310_01.

Tappia, Elena, Gino Marchet, Marco Melacini, and Sara Perotti. 2015. "Incorporating the Environmental Dimension in the Assessment of Automated Warehouses." *Production Planning & Control* 26 (10): 824–838. doi:10.1080/09537287.2014.990945.

Verein Deutscher Ingenieure. 1998. *Durchsatz von Automatischen Lagern mit Gassengebundenen Regalbediensystemen*. 03.100.10; 55.020, No. VDI 4480. Berlin: Beuth-Verlag.

Voß, Michael, Alexander Verl, and Marc Schnierle. 2014. "Automatisierte Energiemanagementsysteme Für Hochregallager: Intelligente Auftragsplanung Zur Steuerung Des Energieniveaus Eines Automatisierten HRL." *Werkstattstechnik Online* 104 (H3): 180–186. Accessed March 31, 2014. http://www.werkstattstechnik.de/wt/get_article.php?data[article_id]=77608

Xu, Xianhao, Guwen Shen, Yugang Yu, and Wei Huang. 2015. "Travel Time Analysis for the Double-Deep Dual-Shuttle aS/RS." *International Journal of Production Research* 53 (3): 757–773. doi:10.1080/00207543.2014.921351.

Zaerpour, Nima, René B. M. de Koster, and Yugang Yu. 2013. "Storage Policies and Optimal Shape of a Storage System." *International Journal of Production Research* 51 (23–24): 6891–6899. doi:10.1080/00207543.2013.774502.